

## Two new geothermal prospects in the Mexican Volcanic Belt: La Escalera and Agua Caliente – Tzitzio geothermal springs, Michoacán, México

Mariana Patricia Jácome-Paz<sup>a,\*</sup>, Daniel Pérez-Zárate<sup>b</sup>, Rosa María Prol-Ledesma<sup>a</sup>, Augusto Antonio Rodríguez-Díaz<sup>a</sup>, Aurora María Estrada-Murillo<sup>a</sup>, Irving Antonio González – Romo<sup>a</sup>, Elizabeth Magaña-Torres<sup>c</sup>

<sup>a</sup> Departamento de Recursos Naturales, Instituto de Geofísica, Universidad Nacional Autónoma de México; Circuito interior s/n, Coyoacán, 04510 Ciudad de México, México

<sup>b</sup> CONACYT-Instituto de Geofísica, Universidad Nacional Autónoma de México; Circuito interior s/n, Coyoacán, 04510 Ciudad de México, México

<sup>c</sup> Escuela Nacional de Estudios Superiores, Unidad Morelia, Universidad Nacional Autónoma de México, 58190, Michoacán, México

### ARTICLE INFO

#### Keywords:

Geothermal energy  
 $\text{CO}_2 - \text{CH}_4$  degassing  
 Fluid geochemistry  
 Isotopes  
 Agua Caliente – Tzitzio  
 La Escalera

### ABSTRACT

The La Escalera and Agua-Caliente Tzitzio geothermal areas are newly discovered geothermal prospects in Mexico that may have the potential to be utilized using binary cycle plants. Hot springs ( $40\text{--}50^\circ\text{C}$ ) are constrained to the river banks in both areas, but gas discharges occur on the banks as well as in the riverbeds. The thermal water is predominantly bicarbonate type. Reconnaissance work yielded encouraging results, as the Na/K geothermometer indicates temperatures between  $139$  and  $245^\circ\text{C}$  for La Escalera water samples in a partial equilibrium. La Escalera and Tzitzio have strong surface gas discharges, and dry gas samples were collected for  $\delta^{13}\text{C}$  isotopic analysis of  $\text{CH}_4$  and  $\text{CO}_2$ ; the results indicate a magmatic origin for the gas discharged.

### 1. Introduction

The recently approved Law for Energetic Sustainability and the approval of the Paris Agreement have raised interest in the development of clean energy technologies and renewable energy sources in Mexico, especially geothermal energy. The interest in the use of geothermal resources in Mexico has promoted the exploration of new geothermal zones as part of the national strategy for the development of clean energy resources. Through the Secretariat of Energy, strategic projects are financed for the exploration of new areas of geothermal interest (Romo-Jones et al., 2017).

The state of Michoacán is an area with abundant hydrothermal activity and is mostly located inside the Mexican Volcanic Belt, a favorable geological environment for geothermal prospects, such as the Los Azufres geothermal field (Pasquaré et al., 1991). Such geothermal activity includes the hot springs discovered in La Escalera and Agua Caliente, municipalities of Charo and Tzitzio, respectively.

During the last decade, few reports on new geothermal prospects, specifically on the chemistry of geothermal fluids in new areas, have been published in Mexico (e.g. Almirudis et al., 2015, 2018; Arango-Galván et al., 2015; Iglesias et al., 2015; Morales et al., 2015; Romo-Jones et al., 2017). The main objective of geochemical exploration in

these areas is to carry out reconnaissance work that includes i) the characterization of hydrothermal fluids discharged in La Escalera and Agua Caliente – Tzitzio geothermal areas, ii) the quantification of the diffuse dynamic degassing of soils and the bubbling springs, and iii) the estimation of the temperatures at depth using chemical geothermometers, which will be of great value to more detailed exploration programs in the future. Additionally, the fluxes of diffuse degassing of  $\text{CO}_2$ ,  $\text{H}_2\text{S}$  and  $\text{CH}_4$  through soil and bubbling springs can be measured and these measurements are powerful tools that can elucidate the origin of the gases and the conditions at depth in the hydrothermal system.

### 2. Geological setting

The Mexican Volcanic Belt (MVB) is a Neogene continental arc with intra-arc extensional tectonics that extends throughout central Mexico and is related to the subduction of the Rivera and Cocos Plates beneath the North American Plate (NAP) at the Middle America Trench (MAT) (Ferrari et al., 2012). Two major fracture zones are subducted beneath west-central southern Mexico along the MAT: the Rivera Fracture Zone (RFZ) and the Orozco Fracture Zone (OFZ) (Blatter and Hammersley, 2010), which are the most recent and the most interesting structural features in this study (Fig. 1). Based on the stationary pole of rotation of

\* Corresponding author.

E-mail address: [jacome@igeofisica.unam.mx](mailto:jacome@igeofisica.unam.mx) (M.P. Jácome-Paz).

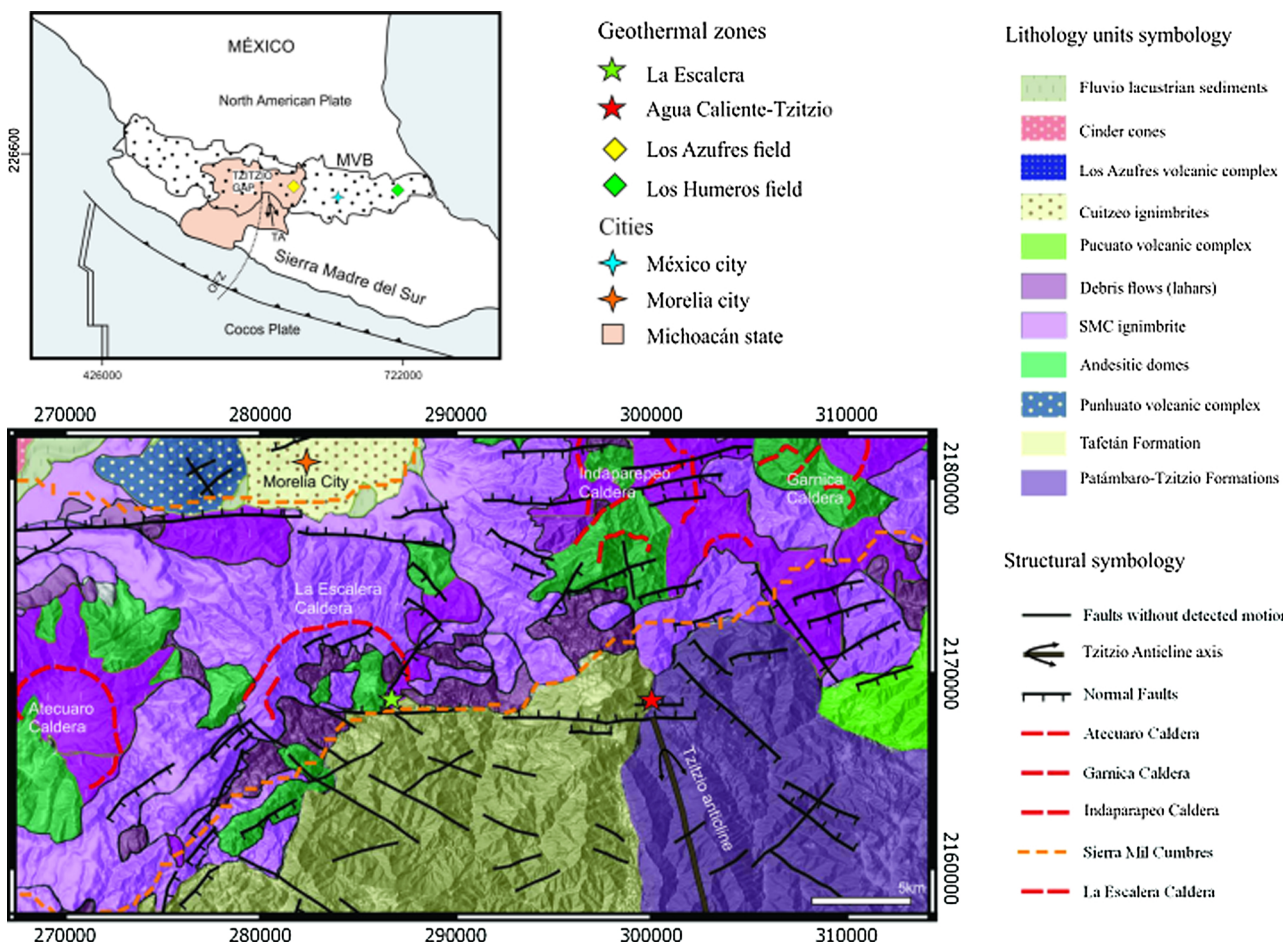


**Fig. 1.** Regional map of the Mexican volcanic belt (MVB), Michoacán state and Tzitzio Gap. Los Azufres and Los Humeros fields are indicated as the nearest geothermal systems to the studied area. Location map of La Escalera and Agua Caliente – Tzitzio geothermal areas south of the SMC, the Sierra de las Mil Cumbres. Main geological units are indicated following Gómez-Vasconcelos et al., 2015; faults without detected motion and normal faults are indicated following Garduño-Monroy et al., 2009.

the Cocos and North American plates and the angle of subduction, the OFZ appears to be constantly subducted beneath the Tzitzio Gap (TG) in the same direction as the Tzitzio anticline on the Earth's surface; therefore, the N-S-trending Tzitzio Anticline bisects the TG (Morán-Zenteno et al., 2007). The “Gap” denomination is due to the lack of active volcanism in the TG, except in the back-arc zone approximately 350 km from the MAT. Several volcanic units from the Early Oligocene to the Middle Miocene make up thick sequences on the margins of the TG and are present as erosional remnants of old volcanic activity within the TG (Pasquaré et al., 1991; Morán-Zenteno et al., 2007; Blatter and Hammersley, 2010).

The La Escalera and Agua Caliente region is located on the southern border of the MVB within the Sierra Madre del Sur (SMS) province (Fig. 1). The La Escalera and Agua Caliente geothermal areas are located within the Tzitzio Gap to the south of the Sierra de las Mil Cumbres (SMC) and Morelia City. The SMC is located within the MVB and neighbors the Los Azufres Geothermal Field to the east, the Michoacán-Guanajuato monogenetic volcanic field to the west, the Cuitzeo Lake basin to the north, and the Balsas River basin to the south. Structurally, the TG is an ENE-trending horst that covers an area of 1022 km<sup>2</sup> (approximately 20 km wide × 60 km long) and contains exposures of chemically bimodal volcanism in the form of ignimbrites, lava domes, lava flows, cinder cones, and related deposits (Gómez-Vasconcelos et al., 2015). The SMC lies unconformably on top of the Patámbaro - Tzitzio Formations to the southeast (Fig. 1). The Patámbaro - Tzitzio Formations include Middle Jurassic-Early Cretaceous conglomerates made up of andesitic clasts, and limestone, schist, and

flysch sequences and Late Cretaceous to Eocene siltstone and sandstone red beds (Pasquaré et al., 1991; Gómez-Vasconcelos et al., 2015). To the southwest, the SMC overlies the Oligocene-Early Miocene Tafetán Formation, which is composed of sedimentary red beds, volcanic conglomerates and basaltic to andesitic lavas (Pasquaré et al., 1991). Approximately 50 km to the SE of the SMC, the Tafetán Formation is intruded by a gabbro dike near Tuzantla, 50 km SE of Tzitzio. This NE-SW-oriented dike is 20 km long and 10 m wide and was dated at  $30 \pm 0.6$  Ma (Gómez-Vasconcelos et al., 2015).

The youngest materials overlying the SMC are the volcanic deposits from the Michoacán-Guanajuato Volcanic Field (MGVF) (Hasenaka and Carmichael, 1987). Four volcanic structures within the SMC range have been identified and dated: the Garnica Volcanic Complex (23 to 17 Ma), the Caldera La Escalera (22.3 to 19.8 Ma), the Caldera de Atécuaro (19.5 to 15.9 Ma) and the Indaparapeo Volcanic Complex (17 to 14 Ma) (Gómez-Vasconcelos et al., 2015).

### 3. Hydrothermal activity

#### 3.1. The La Escalera geothermal area

The La Escalera geothermal area is located southeast of the La Escalera caldera at the intersection of the ENE and WSW regional fault systems (Fig. 1). The area consists of several springs along a river in an approximately 50 m wide area; the springs bubble intensely, water discharge from waterfalls approximately 1 to 4 m high and there is visible red-orange hydrothermal alteration on the rock wall and red and

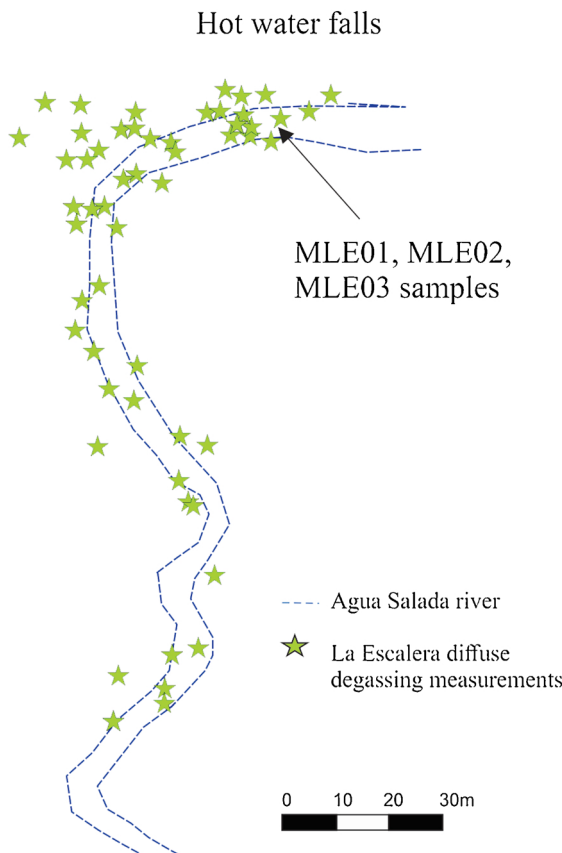


**Fig. 2.** La Escalera thermal area and the locations of diffuse degassing measurements. Blue lines indicate the river direction. A) Examples of warm water falls and hydrothermal alteration on rock walls. B) Measurements of diffuse degassing in soils closer to the waterfalls (For interpretation of the references to colour in this figure legend, the reader is referred to the web version of this article).

green microbial mats (Fig. 2). Temperature measurements were made along the river and high values were detected near all the areas where bubbling springs are visible in the river ( $\sim 50^{\circ}\text{C}$ ), indicating the large area influenced by hydrothermal fluids. Waterfalls feed the river and appear to be the only source of water to the river; therefore, during this exploratory survey it was not possible to identify the springs' sources with certainty.

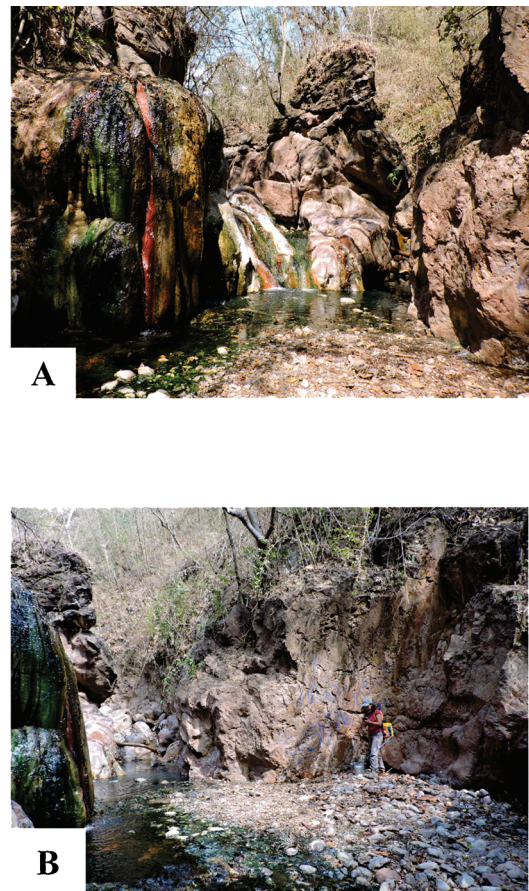
Along the river, 150–200 m downstream, temperatures are between 25 and  $35^{\circ}\text{C}$ , and alteration zones with minor discharges occur. In these areas, some pools have been built for balneology purposes.

The thermal activity occurs in the conglomerates and sandstones of the Patámbaro - Tzitzio Formations, which are overlain by the sandstones and siltstones of the Tafetán Formation and the volcanic rocks of the Escalera Caldera. Mendiola-Pimentel et al. (2017) identified four local fault systems in the thermal zone: NE-SW, NW-SE, E-W and N-S.

### 3.2. The Agua Caliente - Tzitzio geothermal area

The Agua Caliente-Tzitzio geothermal area is in the axis of the Tzitzio anticline, outside the edge of the Caldera La Escalera. Geothermal activity occurs in the boundary between the Tafetán and Patámbaro - Tzitzio Formations, mostly in the sandstones of the Patámbaro – Tzitzio Formation (Fig. 1). Geothermal activity present consists of hot springs and intense bubbling towards the edge of the Patámbaro River and is found in two areas: (a) Agua Caliente north and (b) Agua Caliente south (Fig. 3). This site is within private property in the lowland, at the bottom of a ravine.

The northern area contains more than 15 instances of hydrothermal activity, including strong bubbling in several pools, hydrothermal



alteration (red-green), and two warm water runoffs ( $\sim 30^{\circ}\text{C}$ ). The southern site has a main discharge that has been incased in a metal tube and has a significant regular flow (this main discharge was sampled). Several pools have formed below and around this outflow and present strong bubbling and crusts formed by red hydrothermal alteration.

Similar to the La Escalera geothermal area, four fault systems are present in the thermal zone: the NW-SE, the NE-SW, the NWE-SEW and the N-S systems. The NW-SE system, south of the MVb (Tzitzio region), has mostly lateral movement. The Tzitzio-Valle de Santiago regional fault is a part of this system and produces the Tzitzio fold that was reactivated by right-lateral faults along the Tzitzio Anticline (Garduño-Monroy et al., 2009; Pasquaré et al., 1991).

## 4. Sampling and analytical methods

### 4.1. Soil CO<sub>2</sub> flux survey

A soil CO<sub>2</sub> flux survey at La Escalera and Agua Caliente-Tzitzio was performed during April 11–13, 2017, at the end of the dry season and under stable atmospheric pressure. Soil flux measurements were performed following the accumulation chamber method, using a West Systems instrument and water surface measurements were conducted using a floating chamber. The instrument was equipped with three detectors for CO<sub>2</sub>, CH<sub>4</sub> and H<sub>2</sub>S flux measurements: (1) LICOR LI-800, a nondispersive infrared CO<sub>2</sub> sensor with a detection range of 0.1 to 20,000 ppm/s and an accuracy of < 3% and a reproducibility lower than 10% for the range 0.2 to 10,000 g m<sup>-2</sup> d<sup>-1</sup>; (2) CH<sub>4</sub>-WS infrared, which has a flux detection range from 0.02 to 1444 g m<sup>-2</sup> d<sup>-1</sup>, a 5% accuracy, 2% of repeatability, 22 ppm resolution and a  $\pm 25\%$

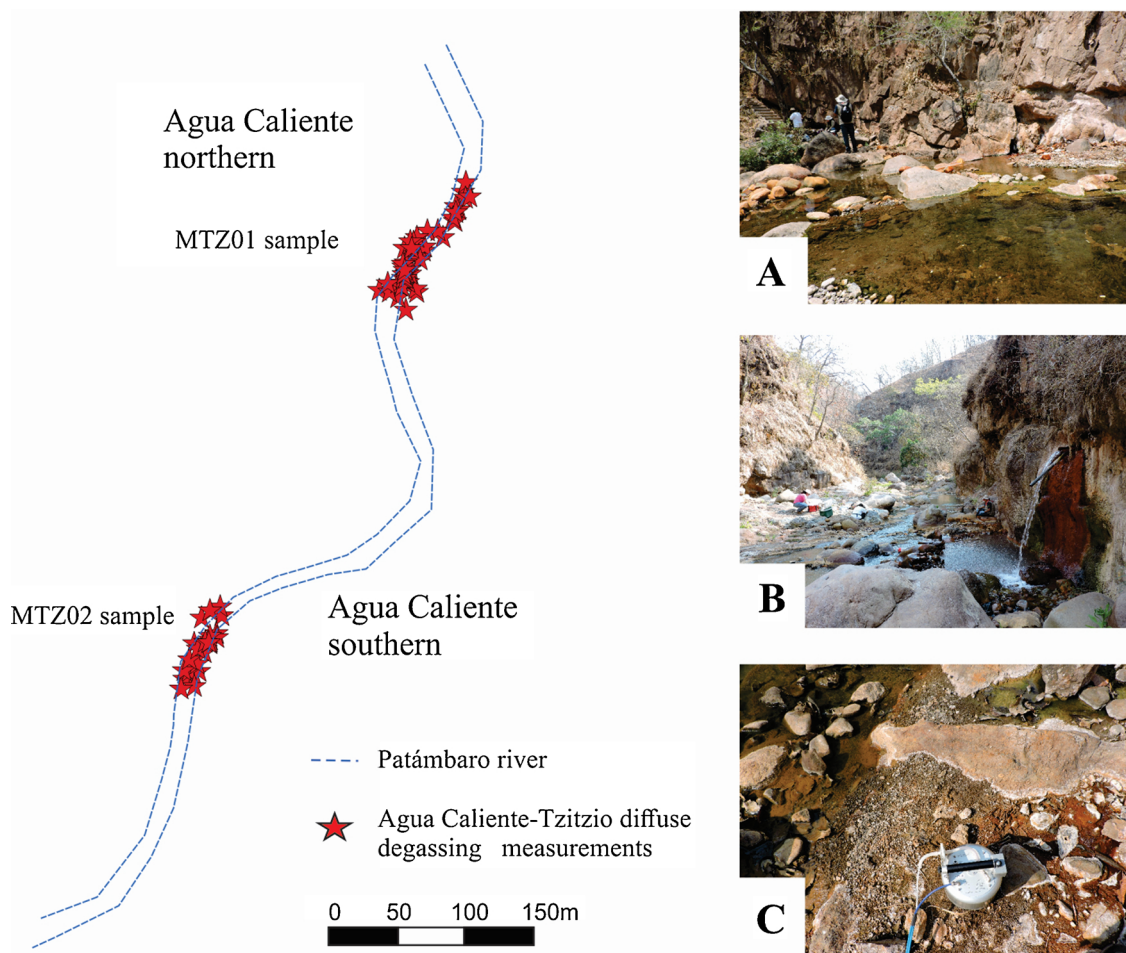


**Fig. 3.** Locations of Agua Caliente diffuse degassing measurements. A) View of Agua Caliente north area. B) View of Agua Caliente south area. C) View of one diffuse degassing measurements in the soil around an example of bubbling water.

precision for the range  $0.1\text{--}5$  moles  $\text{m}^{-2} \text{ d}^{-1}$  and a  $\pm 10\%$  precision for the range  $5\text{--}150$  moles  $\text{m}^{-2} \text{ d}^{-1}$ ; and (3) WEST H<sub>2</sub>S-BH chemical detector, which has a flux detection range from 0.0002 to 0.6 mol  $\text{m}^{-2} \text{ d}^{-1}$ , an accuracy of 3%, a factory calibration of 20 ppm and zero offset  $\leq 0.2$  ppm. Due to the rate of consumption of the detector, the H<sub>2</sub>S flux is systematically 10% underestimated in the accumulation chamber A and 5% underestimated in the accumulation chamber B. In addition, the H<sub>2</sub>S detector is affected by interference sensitivity for several species; therefore, low fluxes can be interpreted to be the result of the interference sensitivity effect (West Systems, 2012).

Two main areas were surveyed at Agua Caliente-Tzitzio, ACTZ01 and ACTZ02, with 50 and 25 points of measurements, respectively. Additionally, 60 measurements were made at La Escalera. Most measurements were carried out at a distance  $< 5$  m, but the grid was modified according to the local topography of the thermal areas, especially in the presence of large boulders, steep slopes and hot soils and water.

The total area of each zone was computed using both GPS coordinates and Wingslib® software. Flux Revision software of the West system, and Wingslib®, Surfer® and Origin® software were used for data postprocessing. The graphical statistical analysis method (GSA) and sequential Gaussian simulations (sGs) were used to compute the total CO<sub>2</sub> flux and to show the total degassing area (Sichel, 1966; Sinclair, 1974; Chioldini et al., 1998; Deutsch and Journeel, 1998; Cardellini et al., 2003a). The GSA method consists of: i) creating a cumulative probability graph with the flux values; (ii) classifying the data into families according to the normality of each family (Sinclair, 1974); (iii) recalculating values for each family; (iv) acquisitioning the statistical parameters of each family; and

(v) calculating the total flux. The total flux is the sum of the fluxes of each family. This method does not consider the spatial distribution of fluxes, it only permits differentiating between different CO<sub>2</sub> degassing mechanisms (e.g. Jácome-Paz et al., 2016).

The sGs method allows the calculation of the total flux and the main degassing alignments show the spatial distribution of the fluxes. The main steps of the sGs method are (i) obtaining the measured fluxes with precise locations in UTM coordinates in a GeoEAS(.dat) format file; (ii) transforming the data into a normal distribution (normal score transformation); (iii) calculating of the experimental and theoretical variograms; (iv) determining the grid and the parameters of the simulation; (v) computing the inverse transformation (back normal score transformation); and (vi) assembling the distribution maps and the total flux calculations. All distribution maps were prepared using a Gaussian simulation, on a grid of  $5 \times 5$  m with 100 simulations for each area.

#### 4.2. Gas sampling and analysis

Bubbling gas samples were collected from thermal springs to determine the isotopic composition of the CO<sub>2</sub> flux using 40 ml vials capped with a pierceable butyl rubber septum. Gas samples obtained were analyzed at the LIE-UNAM (*Laboratorio de Isótopos Estables del Instituto de Geología de la Universidad Nacional Autónoma de México*). For the <sup>13</sup>C analyses, a Finnigan MAT 253 (Thermo Fisher Scientific) mass spectrometer was used and was configured with a dual inlet system and GasBench auxiliary equipment. The GasBench equipment has a Pal autosampler system with a temperature-controlled aluminum plate connected to the spectrometer. The results were reported as  $\delta^{13}\text{C}_{\text{VPDB}}$

using the Vienna Pee Dee Belemnite scale with a standard deviation of 0.2‰, in accordance with Coplen et al. (2006) and Werner and Brand (2001).

#### 4.3. Water sampling and analysis

Water samples for geochemical analysis were collected in 250 ml Nalgene® bottles. The samples collected determine the cations were acidified after collection by adding Suprapure® HNO<sub>3</sub> to attain a pH less than 2. The pH ( $\pm 0.1$  units), electrical conductivity ( $\pm 0.1$  mS/cm), and temperature ( $\pm 0.1^\circ\text{C}$ ) were measured on site using a portable instrument, the Thermo Scientific ORION® A329 model, which was calibrated in the field prior to sampling.

Untreated water samples were collected for anion and stable isotope analyses ( $^{\text{TH}}\text{H}$  and  $^{\text{TO}}\text{O}$ ). Additional samples were collected for the analysis of aqueous SiO<sub>2</sub>, which uses the molybdate spectrophotometric method and a Hach DR-2800 instrument (Hach, 1997). After the samples were collected, CO<sub>3</sub><sup>-2</sup> and HCO<sub>3</sub><sup>-1</sup> were determined on site with a relative standard deviation of less than 1.5% by titration with 0.0232 ± 0.0002 N HCl, using phenolphthalein and methyl orange as indicators.

Major cations and anions in water samples were analyzed at the LIG-UNAM (*Laboratorio de Investigación Geoquímica del Instituto de Geofísica de la Universidad Nacional Autónoma de México*). Analyses of the major cations were performed by ionic chromatography with an ICS-900 Thermo Scientific Dionex™ Ion Chromatograph using analytical and quality assurance procedures for geothermal water chemistry following Pang and Ármannsson (2006). A Dionex analytical column (250 mm × 4 mm ID) and an eluent of 20 mM methanesulfonic acid were used. The ion chromatograph was calibrated with six working cation standards. The analytical precision was  $\pm 3\%$  and the accuracy was higher than 95%. Peaks were identified using Chromeleon™ software. A Metrohm ProFIc-881™ Chromatograph was used for the analyses of major anions. A Metrosep ASupp-7 analytical column (250 mm × 40 mm ID), an MSM-853-MCO suppressor, and an eluent of 3.6 mM Na<sub>2</sub>CO<sub>3</sub> solution were used. The ion chromatograph was calibrated with six working cation standards. The analytical precision was  $\pm 1\%$ . MagicNet™ software was used to identify peaks at an accuracy higher than 95%.

Stable isotope analysis of water was conducted at the LIE-UNAM (*Laboratorio de Isótopos Estables del Instituto de Geología de la Universidad Nacional Autónoma de México*). A Model 908-0008-3001 laser absorption spectrometer from Los Gatos Research was used for the <sup>2</sup>H analysis, while a Thermo MAT 253 mass spectrometer with a Thermo Finnigan GASBENCH II couple interface was used for the analysis of <sup>18</sup>O. The isotope ratios were converted to per mil delta values using the Vienna Standard Mean Ocean Water (Coplen et al., 1983).

## 5. Results and discussion

### 5.1. Geology

#### 5.1.1. La Escalera

Major geological structures, specifically the ring boundary of the Caldera La Escalera and E-W postcaldera faults, and their spatial relationships control the occurrence of the thermal zones. Thermal emanations occur through faults and fractures in reddish sandstones.

The intersections of NE-SW- and E-W-oriented normal and right lateral faults with normal components, and to a lesser extent NW-SE- and NNE-SSW-oriented faults, control the occurrence of thermal activity. The main discharge of the La Escalera spring feeds the Agua Salada River, which is oriented NW-SE.

The NE-SW fault system is extensional and is related to the occurrence of the SMC during the Late Oligocene-Early Miocene. The E-W fault system is related to the intra-arc extension of the MVB, particularly in the thermal region linked to the Morelia-Acambay extensional fault system. The faulting has lateral and mainly extensional behavior, with evidence of recent movement during the Pleistocene to the Holocene. This system also controls the presence of other geothermal systems, e.g., Los Azufres, which is a currently exploited geothermal field to the northeast of La Escalera and Tzitzio (see Fig. 1 for location). Regional extensional faulting in northern and central Mexico trends NW-SE to NNE-SSW and belongs to the Basin and Range province. The activity of these faults began ~30 Ma ago (Henry and Aranda, 1992) and continues today (Garduño-Monroy et al., 2009). In the MVB, these faults may be contemporaneous with the E-W extensional faults (Suter et al., 1995) and in the Tzitzio region this fault system moves laterally (Mennella et al., 2000).

Adjacent to the areas of thermal discharge and bubbling, there are veins, veinlets, crusts, terraces and the presence of pores in rocks filled by calcite, aragonite, quartz, opal, pyrite, celadonite, clays and iron hydroxides. The development of halos from argillic alteration, the presence of travertine and the occurrence of silicic phase veinlets are discrete but abundant along the river. In the geothermal areas, alteration zonation is present between veinlets of silica mineral phases, argillization and travertine deposits.

#### 5.1.2. Agua Caliente-Tzitzio

Major geological structures and their spatial relationships, specifically the NW-SE axis of the Tzitzio Anticline, the NE-SW extensive fault system of the SMC and E-W faults related to the intra-arc extension of the MVB, control the occurrence of the geothermal systems. The intersection of NE-SW- and E-W-oriented normal and right lateral faults with normal components, and, to a lesser extent NW-SE- and NS-oriented faults, controls the occurrence of thermal activity along a NE-SW-oriented stream. The NW-SE system, south of the MVB (Tzitzio region), has a mostly lateral movement. The Tzitzio-Valle de Santiago regional fault is a part of this system and has produced the Tzitzio fold, which was reactivated by right-lateral faults along the Tzitzio Anticline (Garduño-Monroy et al., 2009). This regional structure and its axis is the site of intense faulting, promoting an increase in porosity and permeability in the lithological units of the region, which increases the upwelling of hydrothermal fluids. In the Agua Caliente-Tzitzio geothermal area, faulting is more intense than in the Escalera zone.

Hydrothermal deposits in the region include veins, veinlets and crusts. The mineral association of the deposits consists of quartz, opal, clays, calcite, pyrite and iron hydroxides. Argillization has developed extensively in the sandstones and locally in the matrices of the conglomerates. The veins are banded and composed of quartz and disseminated pyrite. Calcite occurs in veinlets. Oxidation is widely distributed in the area and overlaps the argillization. Alteration present as a zonation similar to that observed in La Escalera, except for in the presence of travertine.

Table 1

Values obtained by the GSA and SGSM techniques for La Escalera thermal spring. For both techniques, the total flux is reported.

Proportion Family (%)	Mean value GSA technique (g m <sup>-2</sup> d <sup>-1</sup> )	Total GSA CO <sub>2</sub> flux (ton d <sup>-1</sup> ) Area : 8125 m <sup>2</sup>	Mean value SGSM technique (g m <sup>-2</sup> d <sup>-1</sup> )	Total SGSM CO <sub>2</sub> flux (ton d <sup>-1</sup> ) Area : 8125 m <sup>2</sup>
Family A 50	14.69	0.06	77.5	
Family B 50	137.69	0.56		
Total flux		0.62		0.63

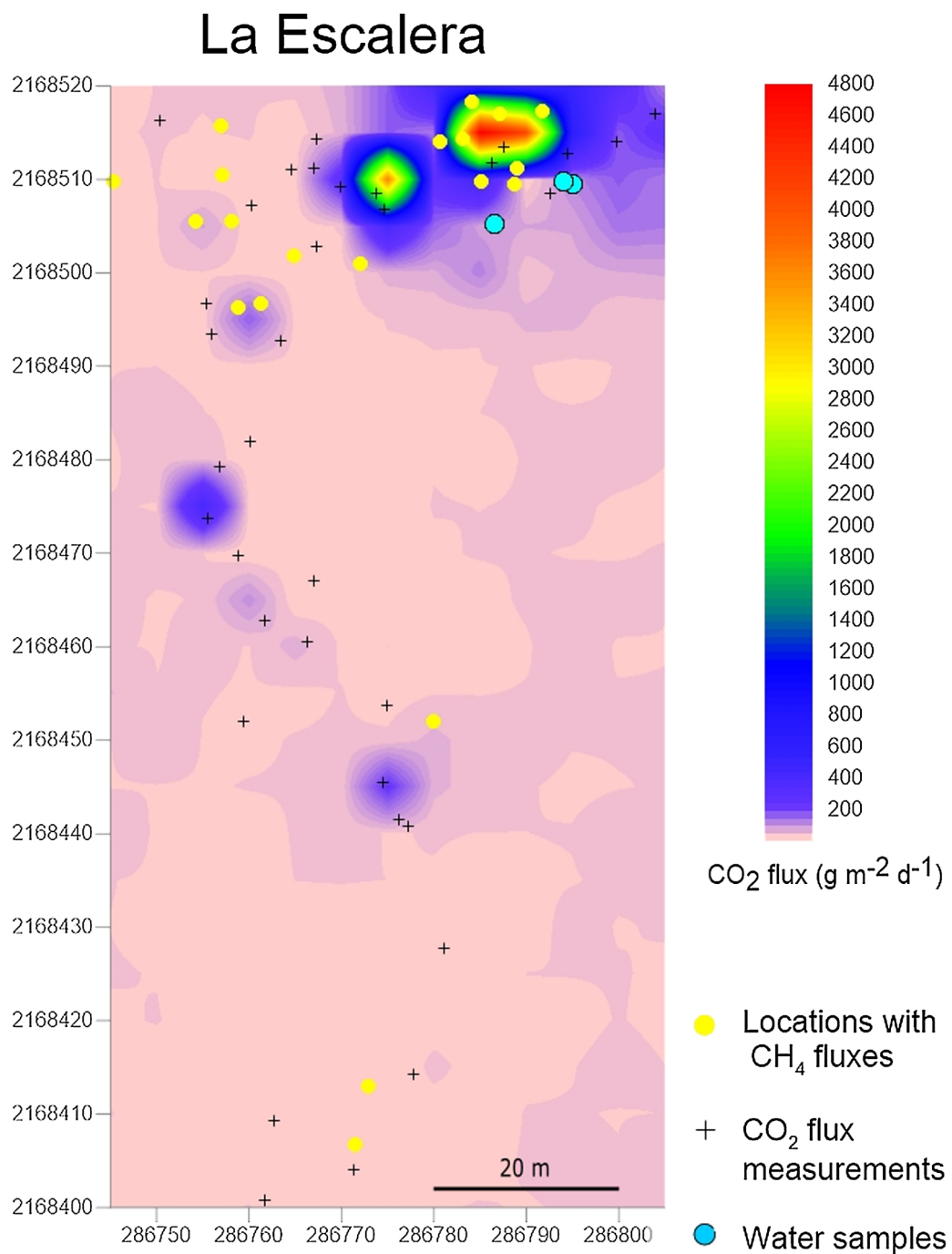


**Fig. 4.** Locations of measurements of CO<sub>2</sub> and CH<sub>4</sub> fluxes, as well as water sample locations. Distribution of CO<sub>2</sub> fluxes obtained by Gaussian simulation at the La Escalera thermal spring.

**Table 2**  
Obtained values for GSA and SGSIM technics for Agua Caliente - North zone.

	Proportion Family (%)	Mean value GSA technique ( $\text{g m}^{-2} \text{d}^{-1}$ )	Total GSA CO <sub>2</sub> flux ( $\text{ton d}^{-1}$ ) Area : 7500 m <sup>2</sup>	Mean value GSIM technique ( $\text{g m}^{-2} \text{d}^{-1}$ )	Total SGSIM CO <sub>2</sub> flux ( $\text{ton d}^{-1}$ ) Area : 7500 m <sup>2</sup>
Family A	70	14.98	0.078	20.41	
Family B	30	84.08	0.18		
Diffusive total flux			0.258		0.15

## Aqua Caliente (North)

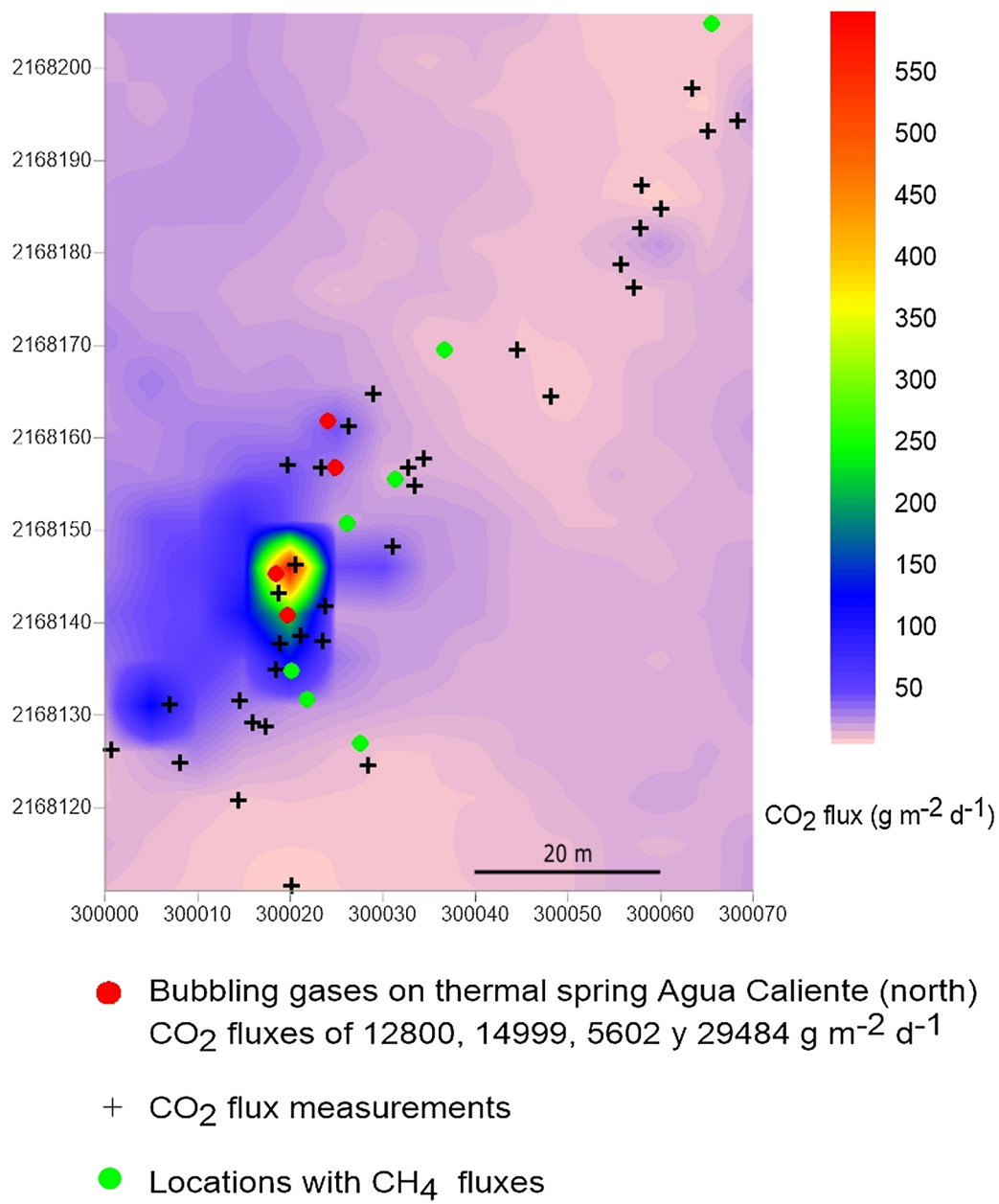


**Fig. 5.** Locations of measurements of  $\text{CO}_2$  and  $\text{CH}_4$  fluxes, as well as water sample locations. Distribution of  $\text{CO}_2$  fluxes obtained by Gaussian simulation at the Aqua Caliente – north thermal spring.

**Table 3**

Values obtained by GSA and SGS techniques for Aqua Caliente - North zone.

Proportion Family (%)	Mean value GSA technique ( $\text{g m}^{-2} \text{d}^{-1}$ )	Total GSA $\text{CO}_2$ flux ( $\text{ton d}^{-1}$ ) Area : 2600 $\text{m}^2$	Mean value SGSIM technique ( $\text{g m}^{-2} \text{d}^{-1}$ )	Total SGSIM $\text{CO}_2$ flux ( $\text{ton d}^{-1}$ ) Area : 2600 $\text{m}^2$
Family A	80	6.53	0.0136	63.98
Family B	20	448.1	0.23	
Total flux		0.24		0.17

### 5.2. Diffuse degassing

#### 5.2.1. La Escalera hot spring

The 60 sites where gas fluxes were measured both in the soil and the water surface yielded  $\text{CO}_2$  flux minimum values of approximately 1  $\text{g m}^{-2} \text{d}^{-1}$ ,

a maximum value of 6090  $\text{g m}^{-2} \text{d}^{-1}$  and a mean value of 352.5  $\text{g m}^{-2} \text{d}^{-1}$ .

According to the GSA technique, the data set can be divided into two degassing families, each of which corresponds to 50% of the measurements (Table 1): family (A) has low values of  $\text{CO}_2$  flux due to

## Aqua Caliente (South)

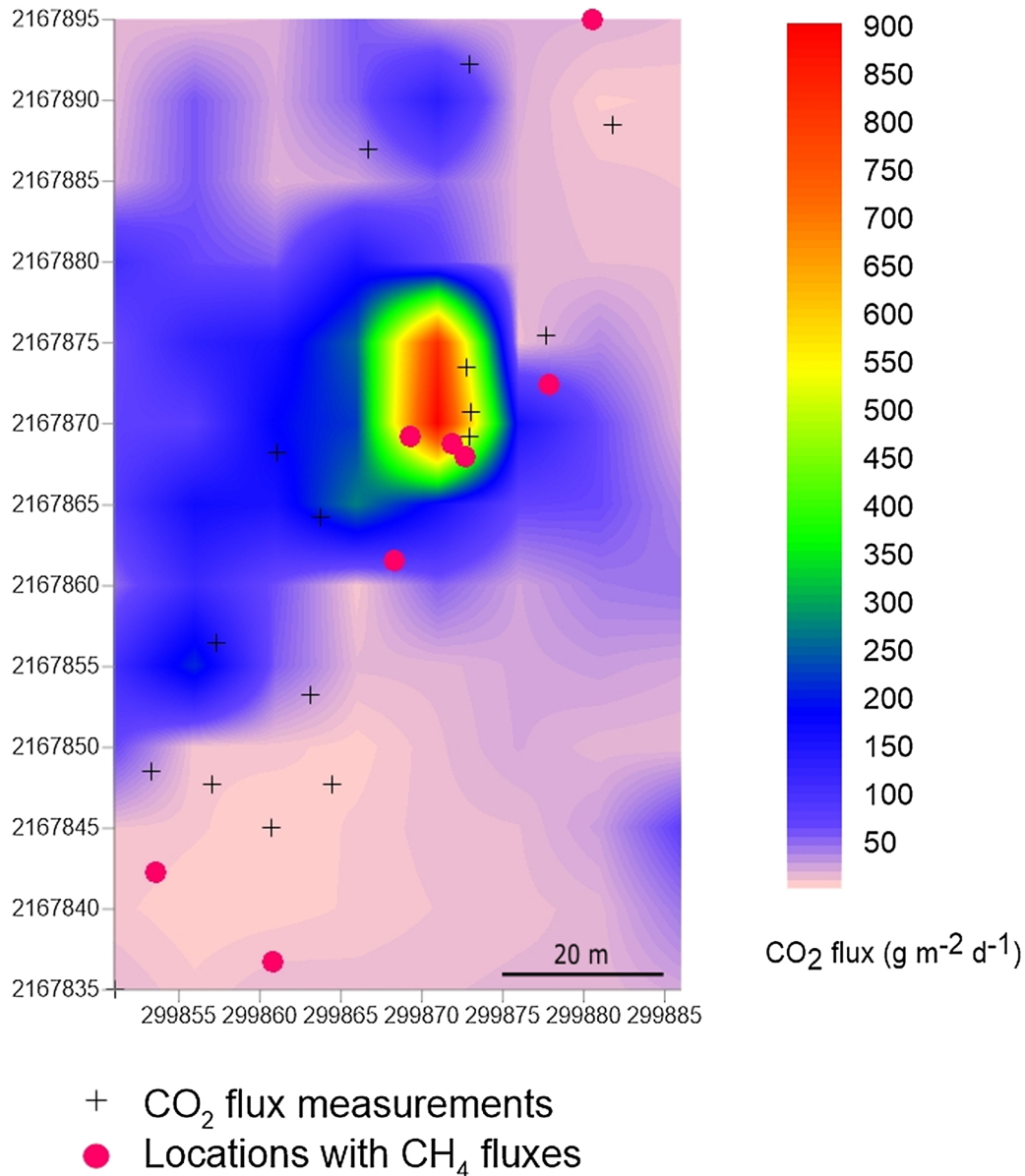


**Fig. 6.** Locations of measurements of CO<sub>2</sub> and CH<sub>4</sub> fluxes, as well as water sample locations. Distribution of CO<sub>2</sub> fluxes obtained by Gaussian simulation at Aqua Caliente – south thermal spring.

**Table 4**

Isotopic composition of water and gas samples from La Escalera and Aguacaliente-Tzitzio hot springs.

Samples	$\delta^{18}\text{O}$	$\delta^2\text{H}$	$\delta^{13}\text{C}$	Description of samples
MLE01	−66.12	−9.31	−8.2	Warm water and bubbling gases
MLE02	−66.09	−9.27	−	Bubbling gases were not observed on site
MLE03	−66.31	−9.26	−	Bubbling gases were not observed on site
MTZ01	−64.93	−9.43	−5.7	Warm water and bubbling gases
MTZ02	−61.57	−8.87	−5.9	Warm water and bubbling gases
MTZ03	−57.72	−7.89	−	Bubbling gases were not observed on site (river waters)

**Table 5**

Chemical characteristics of water samples.

Samples	Sampling location	Sample type	T (°C)	pH	EC (μS/cm)
MLE01	La Escalera	Hot spring water	47.5	6.6	2803
MLE02	La Escalera	Hot spring water	47.6	6.8	2910
MLE03	La Escalera	Hot spring water	50.4	6.6	3023
MTZ01	Aguacaliente-Tzitzio	Hot spring water	41.9	6.2	2167
MTZ02	Aguacaliente-Tzitzio	Hot spring water	38.9	6.6	1584
MTZ03	Aguacaliente-Tzitzio	River water	25.5	8.5	1399

**Table 6**

Chemical analyses (in mg/l) and hydrochemical types of hot water from La Escalera and Agua Caliente-Tzitzio springs (n.d.: not detected; IB: ionic balance).

Samples	SiO <sub>2</sub>	Na <sup>+</sup>	K <sup>+</sup>	Ca <sup>+2</sup>	Mg <sup>+2</sup>	F <sup>-</sup>	Cl <sup>-</sup>	SO <sub>4</sub> <sup>-2</sup>	CO <sub>3</sub> <sup>-2</sup>	HCO <sub>3</sub> <sup>-</sup>	IB%	Hydrochemical types of water
MLE01	35	966	26	73	26	10	848	188	n.d.	1312	-1.4	Na- HCO <sub>3</sub> -Cl
MLE02	41	1332	32	93	33	20	2092	473	n.d.	85	-3.7	Na-Cl
MLE03	45	1776	209	148	55	20	2090	477	n.d.	1472	0.23	Na-Cl
MTZ01	31	960	34	238	69	10	1197	782	n.d.	1058	-6.1	Na-Cl
MTZ02	29	450	22	172	44	5	249	214	n.d.	912	9.7	Na- HCO <sub>3</sub>
MTZ03	25	189	4	34	11	1	9	232	45	280	-1.3	Na- HCO <sub>3</sub>

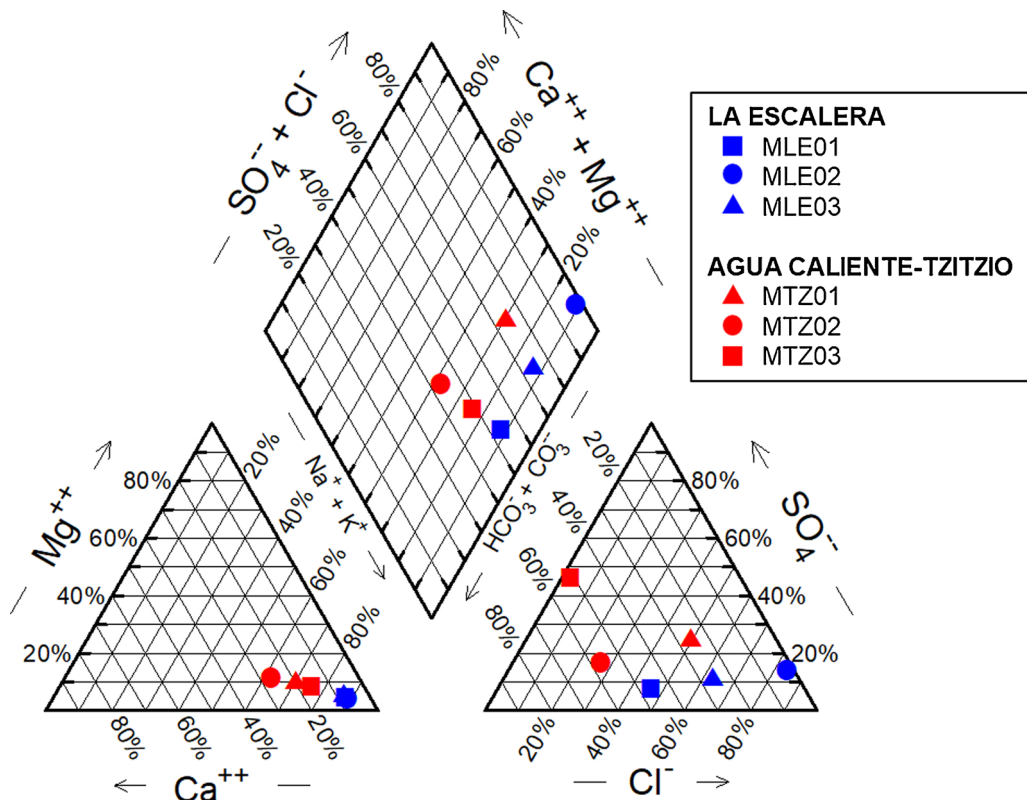


Fig. 7. Piper diagram of water chemical classification for the La Escalera and Agua Caliente- Tzitzio thermal spring waters.

the diffusing process and normal soil respiration, and family (B) has high values of CO<sub>2</sub> flux due to the thermal or anomalous degassing component from intense bubbling on the river surface. The isotope value obtained for bubbling gases was -8.2‰ δC<sup>13</sup> PDB, which appears to confirm the magmatic origin of the thermal degassing (Craig, 1953).

The total flux was calculated using a spherical variogram model with a sill 1 and nugget of 0.5. The grid was made to cover an entire area of 8125 m<sup>2</sup>. The total flux was obtained by Gaussian simulation, and the mean value of each cell of the grid was 0.63 ton d<sup>-1</sup> of CO<sub>2</sub> diffuse flux. The main CO<sub>2</sub> flux distribution pattern is determined by the bubbling zones and degassing along the river; there are no preferential degassing directions indicated by the survey (Fig. 4).

In several locations (30% of the data set) closer to the main waterfall and on the river water surface, significant CH<sub>4</sub> degassing is present (Fig. 4). The values range from 1.6 to 10.5 g m<sup>-2</sup> d<sup>-1</sup>. There is not enough data to construct a distribution map and although the methane flux is relevant, the concentration of CH<sub>4</sub> in the gas samples is below the detection limit; therefore, no carbon isotope analyses could be conducted to determine its origin. However, based on the range of values and the constant fluxes, it could be inferred that methane has a thermogenic origin. There was no diffuse emission of H<sub>2</sub>S within the detection range of the sensor.

#### 5.2.2. Agua Caliente – Northern hot spring

Measurements were made at 50 points on the soil and water surfaces in the Agua Caliente northern area, revealing a CO<sub>2</sub> flux minimum value of 3 g m<sup>-2</sup> d<sup>-1</sup>, a maximum value of 29,484 g m<sup>-2</sup> d<sup>-1</sup> and a mean value of 1427 g m<sup>-2</sup> d<sup>-1</sup>. The cumulative probability plot for the total data set shows two degassing families: the low value family (A) represents 70% of the values, and the high value family (B) represents 30% of the data (Table 2).

The highest values were not used for Gaussian simulation because they must be considered to be outliers. The mean value without the outliers is 66 g m<sup>-2</sup> d<sup>-1</sup>. The variogram model was a spherical variogram with sill 1 and a nugget of 0.3. The grid was made to cover an area of 7500 m<sup>2</sup>. The total CO<sub>2</sub> diffuse flux obtained was 0.15 ton d<sup>-1</sup>.

Both diffusive and advective fluxes must be considered to obtain the total CO<sub>2</sub> flux of the area studied; according to Chiodini et al. (1998), low flux values are governed by diffusion, whereas high values of flux are sustained by advection. The advective flux, in agreement with the GSA method, is represented by the highest flux values (considered to be outliers for simulation and associated with bubbling zones). Using the measured flux and the inferred area (m<sup>2</sup>), advective degassing contributed 0.23 ton d<sup>-1</sup> of flux for the entire area studied. The CO<sub>2</sub> flux distribution map shows a focalized anomalous zone with main degassing in four points and without a significant influence in the surrounding hydrothermal activity area (Fig. 5). The isotope value of carbon (CO<sub>2</sub>) in gas samples is

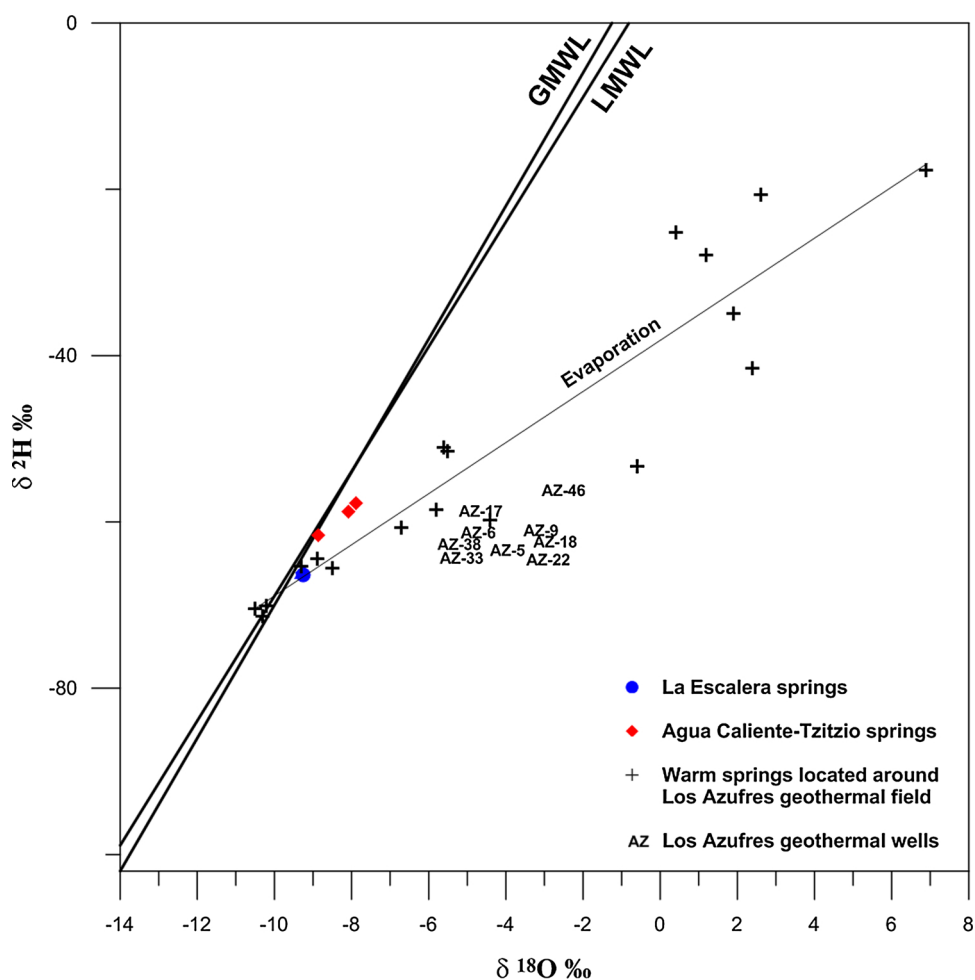


**Fig. 8.** Stable isotope ( $\delta^{18}\text{O}$ ‰ vs  $\delta^2\text{H}$ ‰) diagram of waters from the La Escalera and Agua Caliente-Tzitzio thermal springs. Data are compared with the Global Meteoric Water Line (GMWL; Craig, 1961), the Local Meteoric Water Line (LMWL; Wassenaar et al., 2009), and data reported by González-Partida et al. (2005): geothermal fluids from Los Azufres on geothermal wells and warm springs.

-5.7‰  $\delta\text{C}^{13}$  PDB, which is within the range for fluids of magmatic origin.

In several locations (~ 20% of the data set) closer to the main hot spring and on bubbling zones,  $\text{CH}_4$  degassing (Fig. 3) is present. The  $\text{CH}_4$  flux values range from 2.2 to 5.3  $\text{g m}^{-2} \text{d}^{-1}$ . There are not enough values to construct a distribution map and, similar to La Escalera, the concentration of  $\text{CH}_4$  in gas samples is below the detection limit and thus these samples are not suitable for  $\delta\text{C}^{13}$  analyses. There were no diffuse emissions of  $\text{H}_2\text{S}$  within the detection range of the sensor.

#### 5.2.3. Agua Caliente – Southern hot spring

Twenty-five gas flux measurements were obtained from soil and water surfaces in southern Agua Caliente. The  $\text{CO}_2$  flux data obtained have a minimum value of less than  $1 \text{ g m}^{-2} \text{ d}^{-1}$ , a maximum value of  $1925 \text{ g m}^{-2} \text{ d}^{-1}$  and a mean value of  $227 \text{ g m}^{-2} \text{ d}^{-1}$ . Similar to that of the northern area, the cumulative probability plot shows two degassing families: the low value family (A) represents 80% of the data and the high value family (B) represents 20% of the data (Table 3).

The spherical variogram used to obtain the  $\text{CO}_2$  flux distribution map in the southern Agua Caliente area employed a sill of 1.2 and a nugget of 0.4. The grid covered an area of  $2600 \text{ m}^2$ . The total  $\text{CO}_2$  diffuse flux obtained is  $0.17 \text{ ton d}^{-1}$  (Fig. 6). The isotope value for carbon in bubbling gases is  $-5.9\text{‰ } \delta\text{C}^{13}$  PDB, indicating a magmatic origin.

In several locations (~ 30% of the data) close to the main hot spring and on intense bubbling areas,  $\text{CH}_4$  degassing (Fig. 3) is present, with values from  $4.8$  to  $20.6 \text{ g m}^{-2} \text{ d}^{-1}$ . Data are too scarce to construct a distribution map and the concentration of  $\text{CH}_4$  is below the detection

limit needed to perform the isotope analysis of  $\delta\text{C}^{13}$ , similar to the  $\text{CH}_4$  flux in La Escalera. There was no diffuse emission of  $\text{H}_2\text{S}$  within the detection range of the sensor.

For comparison in both zones, the maximum  $\text{CO}_2$  degassing value (measured in the bubbling areas) can be compared to the measured fluxes in an active and open crater lake, such as the El Chichón Volcano.

The aquifers of the three thermal zones have a high gas contribution, indicating the presence of a degassing thermal source, similar to the crater lakes. The three warm springs show a diffuse degassing mean value of flux similar to that from a neutral volcanic lake, indicated by the ordinary soil respiration from the GSA technique and an advective or anomalous degassing, indicated by bubbling from a magmatic origin, shown by isotope  $\delta^{13}\text{C}$  values (Table 4) in the range of gas of magmatic origin ( $-6.5 \pm 2.5\text{‰}$ ). The values for  $\text{CH}_4$  degassing indicate a high emission in all zones studied. The measured values range from  $1.6$  to  $20.6 \text{ g m}^{-2} \text{ d}^{-1}$ .

Additionally, the  $\text{CH}_4$  fluxes measured with the same accumulation chamber method in the crater area of the volcanic system of Vulcano, Italy ranged from  $0.007$  to  $3.9 \text{ g m}^{-2} \text{ d}^{-1}$ . In Poggio Dell'Olivo, the values ranged from  $0.004$  to  $47.71 \text{ g m}^{-2} \text{ d}^{-1}$  (Cardellini et al., 2003b), at Laki plain the values ranged from  $0$  to  $1.42 \text{ g m}^{-2} \text{ d}^{-1}$ , in the Soudaki geothermal system the values ranged from  $0.04$  to  $29.15 \text{ g m}^{-2} \text{ d}^{-1}$  and in the Pantelleria volcano the values ranged from  $0.03$  to  $3.55 \text{ g m}^{-2} \text{ d}^{-1}$  (D'Alessandro et al., 2006, 2009, 2013).

The significant presence of  $\text{CH}_4$  and  $\text{CO}_2$  anomalous diffuse deep degassing may indicate permeable structures that allow flow from a deep fluid reservoir to reach the shallow warm springs.

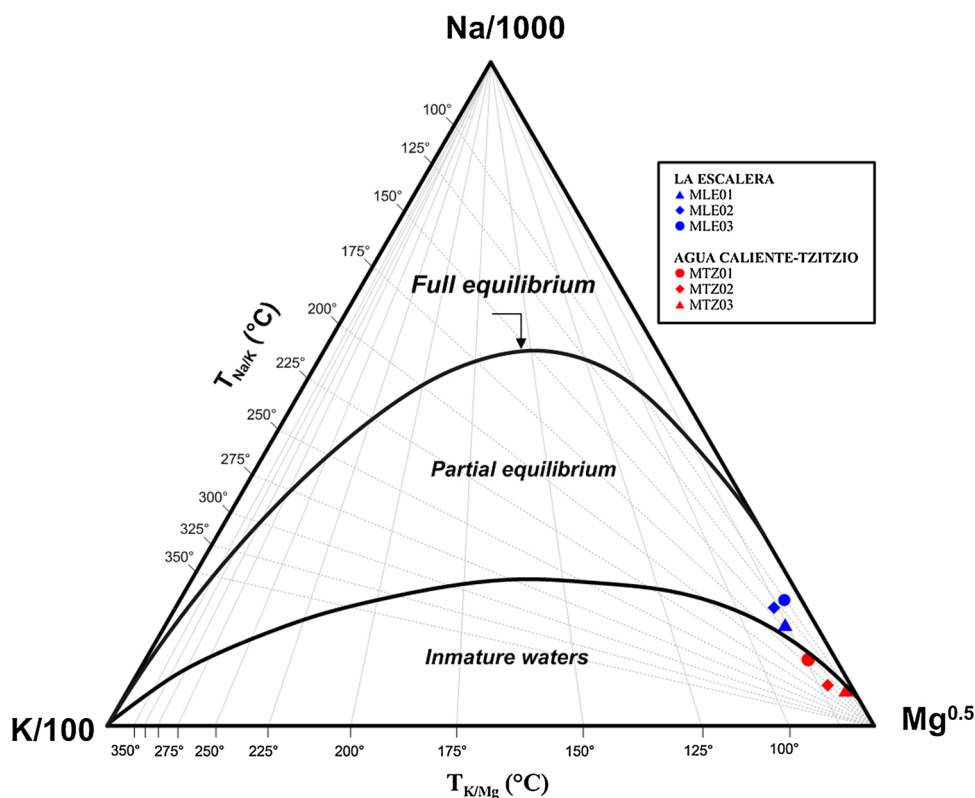


Fig. 9. Giggenbach diagram for Agua Caliente - Tzitzio and La Escalera thermal spring water samples.

### 5.3. Water chemistry

Three water samples were collected from the La Escalera thermal area directly at the bottom of the waterfall in the area where the river starts. All of these samples had a very low salinity and a near to neutral pH.

In Agua Caliente north, only one water sample (MTZ01) was collected from the pools because the site is intensively used for balneology and is contaminated. One additional sample was collected from the Patámbaro River (the MTZ03 water sample). In Agua Caliente south, the water sample was collected from the main outflow (the MTZ02 sample). There is no evidence that this site had been used for balneology as the previous two sites had, but we observed some animals that drank from it.

The physico-chemical parameters for water samples from La Escalera and Agua Caliente-Tzitzio are presented in Table 5. The temperatures of the La Escalera thermal water ranged from 47.5 to 50.4 °C ( $\pm 0.05$  °C), the pH values ranged from 6.6 to 6.8 ( $\pm 0.05$ ), and the electrical conductivity ranged between 2803 and 3023  $\mu\text{S}/\text{cm}$  ( $\pm 0.5$   $\mu\text{S}/\text{cm}$ ). The Agua Caliente-Tzitzio thermal water temperatures ranged from 38.9 to 42 °C ( $\pm 0.05$  °C), the pH ranged from 6.2 to 8.5 ( $\pm 0.05$ ) and the electrical conductivity ranged from 1399 to 2167  $\mu\text{S}/\text{cm}$  ( $\pm 0.5$   $\mu\text{S}/\text{cm}$ ).

The chemical concentrations of the samples analyzed are shown in Table 6 and are plotted in the Piper diagram shown in Fig. 7. The water types present are Na-Cl and Na-bicarbonate. A trend that could be associated with a linear mixing model is not observed in the Piper diagram, indicating that all thermal samples contain the same proportion of thermal and river water end-members.

#### 5.3.1. Water isotope composition

The stable isotope compositions of warm water from the La Escalera and Agua Caliente-Tzitzio springs (Table 4) are plotted in Fig. 8 along the GMWL defined by Craig (1961) and the LMWL defined by Wassenaar et al. (2009). The values obtained show that the samples collected for

this research have an isotopic composition similar to that of meteoric water and no oxygen shift typical of geothermal water. To compare the isotope composition of the La Escalera and Agua Caliente-Tzitzio samples, we included isotopic data for samples from Los Azufres wells and hot springs (González-Partida et al., 2005). We chose Los Azufres because it is the closest geothermal field to those studied here and both its wells and hot springs show a typical pattern for thermal waters: an oxygen shift and evidence for mixing with magmatic water, characteristics which are not present in La Escalera and Tzitzio. The meteoric component predominance in the hydrothermal systems studied can be explained to be the result of a strong dilution with river water, which minimizes the geochemical and isotopic characteristics of the geothermal fluids.

#### 5.3.2. Geothermometry

Application of cation geothermometers requires at least a partial equilibrium in the water-rock interactions; therefore, a ternary Giggenbach plot (Giggenbach, 1988) was used to test equilibrium conditions. La Escalera thermal water samples plot in the partial equilibrium region and Agua Caliente - Tzitzio samples are immature waters (Fig. 9). Therefore, we chose the Na/K geothermometer (Giggenbach, 1988) that is not affected by dilution, to be applied only to the La Escalera samples using the following equation:

$$T(\text{°C}) = \frac{1390}{\log\left(\frac{\text{Na}}{\text{K}}\right) + 1.750} - 273$$

where Na and K concentrations are in mg/kg.

The values obtained were between 139 and 246 °C.

We must assume that the silica concentration is affected by dilution; therefore, the temperatures calculated using the silica geothermometer cannot be considered to be representative of the equilibrium temperature in the geothermal reservoir/aquifer; therefore, we chose to exclude the silica geothermometer evaluation as this will not contribute to the characterization of the geothermal systems.

## 6. Concluding remarks

The La Escalera and Agua Caliente-Tzitzio geothermal areas have warm springs with discharge temperatures of approximately 50 °C and pH values ranging from 6.2 to 8.5. Both thermal zones are hosted in sedimentary rocks of the Late Cretaceous to Eocene Patámbaro - Tzitzio Formations.

The hydrothermal systems are controlled by the interaction of the geological structures of the La Escalera Caldera, the Tzitzio Anticline and the intersections of NE-SW and E-W normal faults related to the intra-arc extension of the MVB.

The first geochemical survey in La Escalera and Agua Caliente-Tzitzio thermal springs provided information about the first chemical classification of waters and the estimation of total CO<sub>2</sub> diffuse degassing. The water of La Escalera and Agua Caliente-Tzitzio north warm springs is of the Na-Cl type, while that of the Agua Caliente-Tzitzio south warm spring is the Na-HCO<sub>3</sub> type.

There is significant CO<sub>2</sub> and CH<sub>4</sub> diffuse degassing, and the isotope analyses suggest the presence of a magmatic component feeding both the La Escalera and Agua Caliente-Tzitzio areas.

The cation geothermometers can be applied only those La Escalera samples that present a partial equilibrium and they yield a wide range of values, from 139 to 246 °C, which is not conclusive. However, it is possible to infer the presence of a medium-low temperature geothermal system in the areas studied because the temperature is likely above 120 °C. These low to medium temperature geothermal resources can be utilized for diverse applications (Lindal, 1973), including power generation using binary cycle power plants and for direct use in agricultural applications.

## Acknowledgments

This work was financially supported by the Mexican Center for Innovation in Geothermal Energy (grant number 207032 CONACyT/SENER) through Project P01. We are grateful to Edith Cienfuegos Alvarado and Francisco J. Otero Trujano for the stable isotope analyses. We thank the two anonymous reviewers and the Prof. Christopher Bromley, who enriched and greatly improved this work through their comments and suggestions.

## References

- Almirudis, E., Guevara, M., Santoyo, E., Torres-Alvarado, I.S., Paz-Moreno, F., 2015. Geothermal energy potential of a promissory Area in the Central and Eastern zones of Sonora, Mexico: a preliminary geochemical study. Proceedings World Geothermal Congress 2015.
- Almirudis, E., Santoyo, E., Guevara, M., Paz-Moreno, F., Portugal, E., 2018. Chemical and isotopic signatures of hot springs from east-central Sonora state (Mexico): a new prospection survey of promissory low-to-medium temperature geothermal systems. Rev. Mex. Cienc. Geolá³gicas 35 (2), 116–141.
- Arango-Galván, C., Prol-Ledesma, R.M., Torres-Vera, M.A., 2015. Geothermal prospects in Baja California peninsula. Geothermics. 55, 39–57.
- Blatter, D.L., Hammersley, L., 2010. Impact of the Orozco fracture zone on the central Mexican Volcanic Belt. J. Volcanol. Geotherm. Res. 197, 67–84.
- Cardellini, C., Chiodini, G., Frondini, F., 2003a. Application of stochastic simulation to CO<sub>2</sub> flux from soil: mapping and quantification of gas release. J. Geophys. Res. 108, 2425. <https://doi.org/10.1029/2002JB002165>.
- Cardellini, C., Chiodini, G., Frondini, F., Granieri, D., Lewicki, J., Peruzzi, L., 2003b. Accumulation chamber measurements of methane fluxes: application to volcanic-geothermal areas and landfills. Appl. Geochem. 18, 45–54.
- Chioldini, G., Cioni, R., Guidi, M., Raco, B., Marini, L., 1998. Soil CO<sub>2</sub> flux measurements in volcanic and geothermal areas. Appl. Geochem. 13, 543–552. [https://doi.org/10.1016/S0883-2927\(97\)00076-0](https://doi.org/10.1016/S0883-2927(97)00076-0).
- Coplen, T.B., Kendall, C., Hopple, J., 1983. Comparison of stable isotope reference samples. Nature 302, 236–238.
- Coplen, T., Brand, W.A., Gehre, M., Grönning, M., Meijer-Harro, A.J., Toman, B., Erkouteren, R.M., 2006. New guidelines for  $\delta^{13}\text{C}$  measurements. Anal. Chem. 78, 2439–2441.
- Craig, S., 1953. The Geochemistry of stable carbon isotopes. Geochim. Cosmochim. Acta 3, 53–92.
- Craig, H., 1961. Isotopic variations in meteoric waters. Science 133, 1702–1703. <https://doi.org/10.1126/science.133.3465.1702>.
- D'Alessandro, W., Brusca, L., Kyriakopoulos, K., Rotolo, S., Michas, G., Minio, M., Papadakis, G., 2006. Diffuse and focussed carbon dioxide and methane emissions from the Sousaki geothermal system, Greece. Geophys. Res. Lett. 33, L05307.
- D'Alessandro, W., Bellomo, S., Brusca, L., Fiebig, J., Longo, M., Martelli, M., Pecorino, G., Salerno, F., 2009. Hydrothermal methane fluxes from the soil at Pantelleria island (Italy). J. Volcanol. Geotherm. Res. 187, 147–157.
- D'Alessandro, W., Gagliano, A.L., Kyriakopoulos, K., Parello, F., 2013. Hydrothermal Methane Fluxes from the Soil at Lakki Plain (Nisyros Island, Greece), vol XLVII Bulletin of the geological society of Greece.
- Deutsch, C.V., Journel, A.G., 1998. GSLIB: Geostatistical Software Library and Users Guide, 2nd ed. Oxford University Press, New York.
- Ferrari, L., Orozco-Esquível, M.T., Manea, V., Manea, M., 2012. The dynamic history of the Trans-Mexican Volcanic Belt and the Mexico subduction zone. Tectonophysics. <https://doi.org/10.1016/j.tecto.2011.09.018>. Invited review paper.
- Garduño-Monroy, V.H., Pérez-López, R., Israde-Alcántara, I., Rodríguez-Pascua, M.A., Szynkaruk, E., Hernández-Madrigal, V.M., García-Zepeda, M.L., Corona-Chávez, P., Ostrovskiy, M., Medina-Vega, V.H., García-Estrada, G., Carranza, O., Lopez-Granados, E., Mora-Chaparro, J.C., 2009. Paleoseismology of the southwestern Morelia-Acabay fault system, central Mexico. Geofis. Int. 48, 319–335.
- Giggenbach, W.F., 1988. Geothermal solute equilibria: derivation of Na-K-Mg-Ca geoindicators. Geochim. Cosmochim. Acta 52 (12), 2749–2765.
- Gómez-Vasconcelos, M.G., Garduño-Monroy, V.H., Macías, J.L., Layer, P.W., Benowitz, J.A., 2015. The Sierra de Mil Cumbres, Michoacán, México: Transitional volcanism between the Sierra Madre Occidental and the Trans-Mexican volcanic belt. J. Volcanol. Geotherm. Res. 301, 128–147. <https://doi.org/10.1016/j.jvolgeores.2015.05.005>.
- González-Partida, E., Carrillo-Chávez, A., Levresse, G., Tello-Hinojosa, E., Venegas-Salgado, S., Ramírez-Silva, G., Pal-Verma, M., Tritilla, J., Camprubi, A., 2005. Hydrogeochemical and isotopic fluid evolution of the Los Azufres geothermal field. Central Mexico. Appl. Geochem. 20, 23–39.
- Hach, 1997. Portable laboratory manual. Loveland, CO, USA.
- Hasenaka, T., Carmichael, I.S.E., 1987. The cinder cones of Michoacán-Guanajuato, Central Mexico: petrology and chemistry. J. Petrol. 28, 241–269.
- Henry, C.D., Aranda, J.J., 1992. The real southern Basin and Range: mid- to late Cenozoic extension in México. Geology 20, 701–704.
- Iglesias, E.R., Torres, R.J., Martínez-Estralla, J.I., Reyes-Picasso, N., 2015. Summary of the 2014 assessment of medium- to low-temperature Mexican geothermal resources. Proceedings World Geothermal Congress 2015, 16081 7pp.
- Jácome-Paz, M.P., Ingaggiati, S., Taran, Y., Vita, F., Pecorino, G., 2016. Carbon dioxide emissions from Speccchio di Venere, Pantelleria, Italy. Bull. Volcanol. 78, 29. <https://doi.org/10.1007/s00445-016-1023-6>.
- Lindal, B., 1973. Industrial and other applications of geothermal energy. In: Armstead, H.C.H. (Ed.), Geothermal Energy. UNESCO, Paris, pp. 135–148.
- Mendiola-Pimentel, L.A., Garduño-Monroy, V.H., Jiménez-Haro, A., Guevara-Alday, J.A., 2017. Structural geology of the La Escalera geothermal area, Michoacán, Mexico. Proceedings of the 2017 Annual Meeting of UGM.
- Mennella, L., Garduño, V.H., Bonassi, O., 2000. Fault-slip analysis in the basal units of the Mexican Volcanic Belt on the eastern flank of the Tzitzio Anticline, Michoacán, Mexico. GSA Special Paper Cenozoic Tectonics and Volcanism of Mexico 334, 237–246.
- Morales, J.I., Villanueva-Estrada, R.E., Rodríguez, R., Armienta, M.A., 2015. Geological, hydrogeological and geothermal factors associated to the origin of arsenic, fluoride, and groundwater temperature in a volcanic environment “Bajío Guanajuatense”. Environ. Earth Sci. <https://doi.org/10.1007/s12665-015-4554-9>.
- Morán-Zenteno, D.J., Cercia, M., Keppie, J.D., 2007. The Cenozoic tectonic and magmatic evolution of southwestern México: advances and problems of interpretation. In: Alániz-Álvarez, S.A., Nieto-Samaniego, A.F. (Eds.), Geology of México: Celebrating the Centenary of the Geological Society of México: Geological Society of America Special Paper 422, pp. 71–91. [https://doi.org/10.1130/2007.2422\(03](https://doi.org/10.1130/2007.2422(03).
- Pang, Z., Ármannsson, H. (Eds.), 2006. Analytical Procedures and Quality Assurance for Geothermal Water Chemistry 1 UNU-GTP, Iceland Report, 172 pp.
- Pasquaré, G., Ferrari, L., Garduño, V.H., Tibaldi, A., Vezzoli, L., 1991. Geologic Map of the Central Sector of the Mexican Volcanic Belt, States of Guanajuato and Michoacán, Mexico, map and Chart Series MCH072. The Geological Society of America, U. S. A.
- Romo-Jones, J.M., Gutiérrez-Negrín, L.C.A., Flores-Armenta, M., del Valle, J.L., García, A., 2017. 2016 Mexico Country Report IEA Geothermal. 10 pp. .
- Sichel, H.S., 1966. The estimation of means and associated confidence limits for small samples from lognormal populations. Proceedings Symposium a Mathematical Statistics and Computer Applications in Ore Valuation 106–122.
- Sinclair, A.J., 1974. Selection of threshold values in geochemical data using probability graphs. J. Geochem. Explor. 3, 129–149.
- Suter, M., Quintero, O., López, M., Aguirre, G., Farrar, E., 1995. The Acambay graben: active intraarc extension in the trans-Mexican volcanic belt, Mexico. Tectonics 14, 1245–1262.
- Wassenra, L.I., Van Wilgenburg, S.L., Larson, K., Hobson, K.A., 2009. A groundwater isoscapes (8D,  $\delta^{18}\text{O}$ ) for Mexico. J. Geochem. Explor. 102, 123–136.
- Werner, R.A., Brand, W.A., 2001. Referencing strategies and techniques in stable isotope ratio analysis. Rapid Commun. Mass Spectrom. 15, 501–519.
- West Systems, 2012. Portable Diffuse Flux Meter With Li-COR CO<sub>2</sub> Detector, Handbook. West Systems srl, Italy.